Structural Engineering and Mechanics, *Vol. 68, No. 5 (2018) 519-526*
DOI: https://doi.org/10.12989/sem.2018.68.5.519

Experimental training of shape memory alloy fibres under combined thermomechanical loading

Digamber Shinde[1a], Pankaj V Katariya[2b], Kulmani Mehar[2c], Md. Rajik Khan[1d], Subrata K Panda[*2] and Harsh K Pandey[3e]

[1]Department of Industrial Design, NIT Rourkela, Rourkela-769008, Odisha, India
[2]Department of Mechanical Engineering, NIT Rourkela, Rourkela-769008, Odisha, India
[3]Dr. C.V. Raman Institute of Science & Technology, Kargi Road, Bilaspur-495113, Chhattisgarh, India

(Received July 25, 2018, Revised August 6, 2018, Accepted August 26, 2018)

Abstract. In this article, experimental training of the commercial available shape memory alloy fibre (SMA) fibre under the combined thermomechanical loading is reported. SMA has the ability to sense a small change in temperature (≥10°C) and activated under the external loading and results in shape change. The thermomechanical characteristics of SMA at different temperature and mechanical loading are obtained through an own lab-scale experimental setup. The analysis is conducted for two types of the medium using the liquid nitrogen (cold cycle) and the hot water (heat cycle). The experimental data indicate that SMA act as a normal wire for Martensite phase and activated behavior i.e., regain the original shape during the Austenite phase only. To improve the confidence of such kind of behavior has been verified by inspecting the composition of the wire. The study reveals interesting conclusion i.e., while SMA deviates from the equiatomic structure or consist of foreign materials (carbon and oxygen) except nickel and titanium may affect the phase transformation temperature which shifted the activation phase temperature. Also, the grain structure distortion of SMA wire has been examined via the scanning electron microscope after the thermomechanical cycle loading and discussed in details.

Keywords: shape memory alloy (SMA); thermo-mechanical cycle (TMC); martensite transformation; phase change; liquid nitrogen (LN2)

1. Introduction

Shape Memory Alloy (SMA) have high power to weight ratio and solid-state smart material that tends to regain back to their original shape, these phenomena take place upon either heating or cooling according to the recrystallisation temperature. This, in turn, eliminate the conventional actuators. Uchil *et al*. (1999) observed the shape memory effect or the super-elasticity of SMA properties during the solid phase transformation i.e., the molecular rearrangement. There are two main phases in SMA, high temperature parent phase named as austenite whereas the low temperature phase is martensite. The phase obtained during the transformation between austenite to martensite refers to martensite phase transformation, this kind of effect is called, Shape Memory Effect (Lobo *et al.* 2015). The equiatomic SMA (50% Ni-50% Ti by weight) is known as Nitinol which has the intermediate phase of austenite and martensite as intermediate R phase. Nitinol has the body-centered cubic (BCC) structure in high temperature phase, monoclinic unit cell in low temperature phase and it has rhombohedral crystallites in its intermediate phase (Nath *et al.* 2017). The NiTi SMAs are very sensitive to thermo-mechanical load and corresponding alloy composition, which affects the final properties. However, the properties can be changed according to the process parameters of shape memory i.e., composition, annealing temperature/time and cold work (Saikrishna *et al.* 2001, Cuellar *et al.* 2016, Stosic *et al.* 2017). A normal SMA actuator has the potential to exchange complex electromechanical systems, thereby reducing the size, cost and weight. The compactness of SMAs allows it to combine without difficulty with the mechanical devices of small size and used as the actuating elements (Koomen 2015). The only restriction of SMA related to the energy efficiency and time response limits, while associated with various advantages like high strain recovery rate, silent operation, zero-gravity environment, spring characteristics and can be formed as wires, plate, etc. including the flexibility. Due to the availability of various forms, SMA has wide range of application in the mainstream industries like aircraft and

*Corresponding author, Associate Professor
E-mail: call2subrat@gmail.com or pandask@nitrkl.ac.in
[a]M. Tech Scholar
E-mail: shinde.digamber44@gmail.com
[b]Ph.D. Scholar
E-mail: pk.pankajkatariya@gmail.com
[c]Ph.D. Scholar
E-mail: kulmanimehar@gmail.com
[d]Assistant Professor
E-mail: mdrajik25@gmail.com
[e]Associate Professor
E-mail: harsh25pandey@gmail.com

ISSN: 1225-4568 (Print), 1598-6217 (Online)

spacecraft, military, automotive, robotics, civil structures, telecommunication, biomedicine, engines including the crafts (Antunes *et al.* 2018). SMA wire when undergoes repeated temperature variation cycles through the transformation range under a constant or varying load, this referred as the thermo-mechanical cycling (TMC). It is noticed that major functional properties such as strain response, transformation temperature, transformation hysteresis, etc. keeps changing frequently upon the TMC for SMA (Bhaumik *et al.* 2008, Ramaiah *et al.* 2005, Saikrishna *et al.* 2006, Eggeler *et al.* 2004, Humbeeck 1991, Stachowiak and McCormick 1988, Perkins and Sponholz 1984). In addition, it is also observed that the unstable behavior is responsible to generate the defects in the microstructure during TMC (Bhagyaraj *et al.* 2013, Liu *et al.* 1999, Jiang *et al.* 1997, Stalmans *et al.* 1991). The response of the TMC in SMA largely depends on the material composition, stress-strain region of TMC and the thermo-mechanical processing history (Erbstoeszer *et al.* 2000). In order to examine the thermo-mechanical behaviour of SMA wire an experimental setup was developed in the past (Churchill and Shaw 2008). For analysis purpose, the SMA wire clamped under 100N load to achieve the mechanical loading whereas the heating cycle was done by using an electrical resistive heating and natural convection. The major limitation of this setup was fixed loading and restricted to types of wires. In addition, the setup was unable to give accurate results for the studies below the room temperature. The structural application of different smart materials and the corresponding numerical analysis of the hybrid structures are provided exclusively (Arani *et al.* 2011, Barkozi *et al.* 2012, Arani and Kolahchi 2016, Baseri *et al.* 2016, Bilouei *et al.* 2016, Kolahchi and Bidgoli 2016, Kolahchi *et al.* 2016a, 2016b, Hajmohammad *et al.* 2017, Kolahchi 2017, Kolahchi and Cheraghbak 2017, Kolahchi *et al.* 2017a, 2017b, 2017c, Zamanian *et al.* 2017, Zarei *et al.* 2017, Amnieh *et al.* 2018, Golabchi *et al.* 2018, Hajmohammad *et al.* 2018a, 2018b, 2018c) using various numerical techniques. Likewise, a series of study (Bouderba *et al.* 2016, Bousahla *et al.* 2016, Hamidi *et al.* 2015, Khetir *et al.* 2017, El-Haina *et al.* 2017, Menasria *et al.* 2017, Chikh *et al.* 2017, Mouffoki *et al.* 2017, Attia *et al.* 2018, Karami *et al.* 2018) are provided in the open literature to show the effect of thermomechanical loading on the advanced structures or the structural components. Taghizadeh et al. (2015) examined the bending responses of the beam based on nonlocal finite element method (NL-FEM). The nonlinear dynamic buckling responses of the smart (piezo) composite plate is investigated by Totounferoush *et al.* (2014) usingthye Reddy's theory. In recent past, a four-variable refined plate theory is developed by Tounsi and co-authors (2016a, 2016b, 2016c) to investigate the thermo-mechanical bending, bucking and post-buckling responses of the FGM sandwich structures.

Based on the above literature survey, it is understood that the activation of SMA wires under the combined thermomechanical load including the low-temperature effect (liquid nitrogen) not reported in the open literature. Hence, the present research aims to fabricate two experimental set-up for the training as well as the TMC behaviour of the commercially available SMA fibre using two kinds of treatment i.e., cold (liquid nitrogen) and the hot water. Further, the grain structure of the SMA wire and the molecular rearrangement due to the thermomechanical loading have been examined via the scanning electron microscope (SEM). Additionally, all three commercial SMA wire compositions are verified via SEM to indicate the necessary reason related to their corresponding actuation. Finally, the composition and the combined loading effect have been explored with respect to their stable state temperatures (Austenite or Martensite) under the combined temperature and mechanical loading.

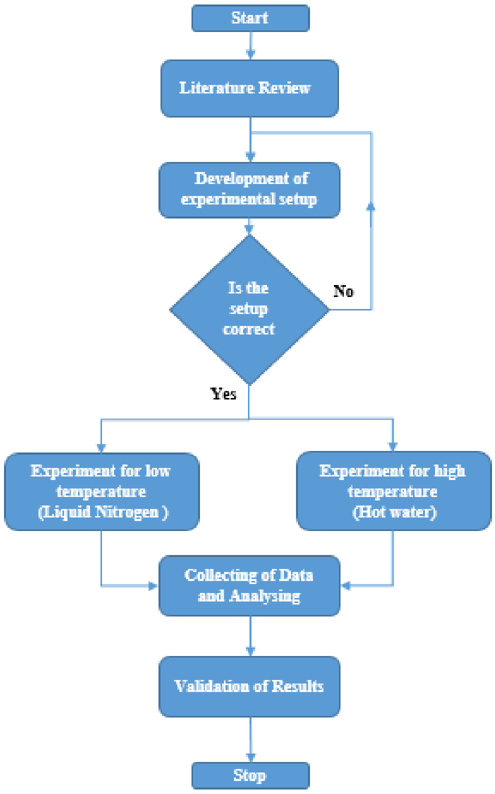

Fig. 1 Development of an experiment set-up

2. Experimental set-up

In the present work, the experimental set-up is developed to analyse the behavior of the SMA wire under different conditions at National Institute of Technology Rourkela, India. To establish the experimental test rig for the said training of the commercially available SMA wires and the corresponding data acquisition details provided in Fig. 1.

The test bench facility is developed to perform the desired experiment using two different medium i.e., the liquid nitrogen and the hot water. The setup consists of actuation unit (low temperature and high temperature), mechanical loading unit, sensors unit, microcontroller board, Parallax Data Acquisition tool (PLX-DAQ) along with computer unit. In order to perform the TMC at a lower temperature, the liquid nitrogen has been passed in the cold

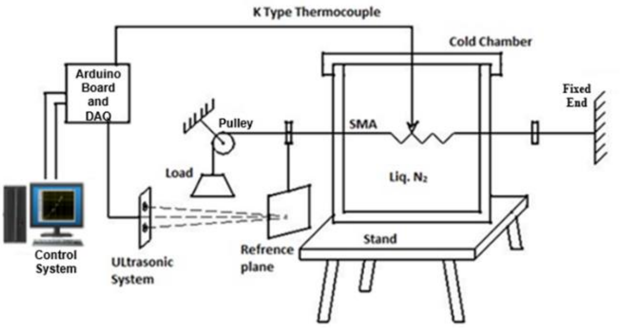

Fig. 2 Sketch of setup for liquid nitrogen actuation

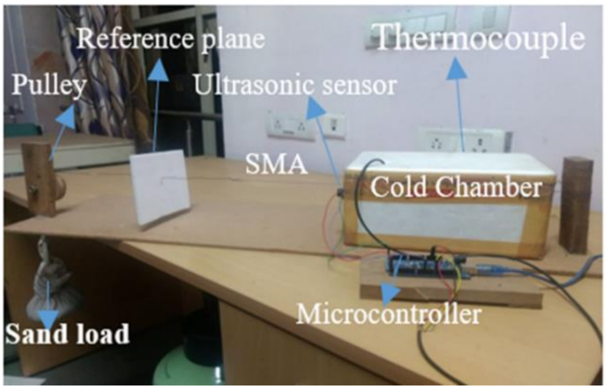

Fig. 3 Sketch of setup for liquid nitrogen actuation

chamber whereas the TMC at a higher temperature has been achieved by varying the temperature of water bath through an external source. In both the cases, the mechanical cycle is attained via the sand load at 7N using the pulley can be seen in Fig. 2.

For measurement of displacement, ultrasonic sensor HRLV-MaxSonar-EZ has been used. The operating voltage of the sensor is from 2.5 V to 5.5 V and pulse width is 1uS/mm. This sensor is the most cost-effective when the precision range finding and low-voltage are applied. For measurement of temperature in Celsius (°C) K-type thermocouple is used. This thermocouple has an operating temperature range from −270°C to 1,260°C. The microcontroller (Arduino mega 2560) having 54 digital input/output pins and 16 MHz crystal oscillator is used to connect the sensors and Parallax Data Acquisition tool (PLX-DAQ). PLX-DAQ is a software add-in for Microsoft Excel, it drops all the data in a proper manner as received from the microcontroller.

2.1 Liquid nitrogen actuation

The experimental set-up for liquid nitrogen actuation has been developed and the schematic line diagram is shown in Fig. 2 and the laboratory based experimental set-up is presented in Fig. 3. The SMA wire is subjected to cold temperature by passing it through the cold chamber, where the liquid nitrogen is responsible to create lower temperature inside the cold chamber. Hence, the cooling process is achieved via liquid nitrogen and the heating process by natural convection. The cooling and the heating TMC is performed for three trials at 7N mechanical loading

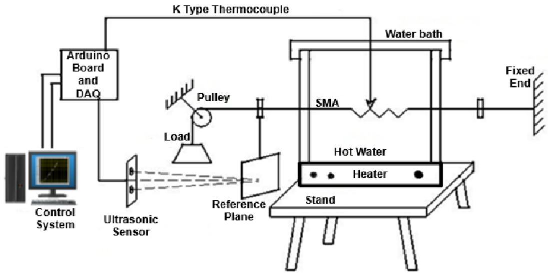

Fig. 4 Sketch of setup for hot water actuation

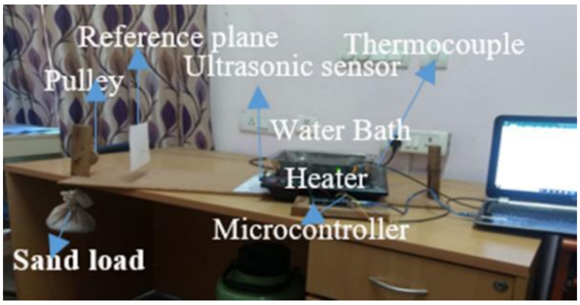

Fig. 5 Experimental set-up for hot water actuation

and the data is recorded within the temperature range for maximum displacement.

After verifying that all the sensors are stable the experiments are conducted. The SMA wire is passed through the cold chamber, its one end is fixed and the other end is subjected to the sand load over a pulley. The liquid nitrogen is passed into the cold chamber, which is subjected to the martensite phase after a while the SMA wire is exposed to the atmosphere, where the temperature of the SMA wire returns back to the atmospheric temperature by natural convection. Similarly, the cycle is repeated for three experimentation trials. The microcontroller collects the reading in terms of emf and pulse from the temperature sensors and ultra-sonic sensor, respectively and this data is observed in PLX-DAQ in terms of temperature (°C) and displacement (mm), respectively.

2.2 Hot water actuation

In order to perform the experiment via hot water actuation, the hot water bath is placed instead of the cold chamber which has been used for the liquid nitrogen actuation as shown earlier in Fig. 2. The schematic line diagram for hot water actuation is shown in Fig. 3 and the experimental set-up is presented in Fig. 4. The SMA wire is actuated using the hot water in water bath via an external heating source and the cooling is achieved by natural convection.

3. Results and discussion

3.1 Liquid nitrogen actuation

In this section, the experiments are performed on SMA wire for 7N mechanical loading via liquid nitrogen using

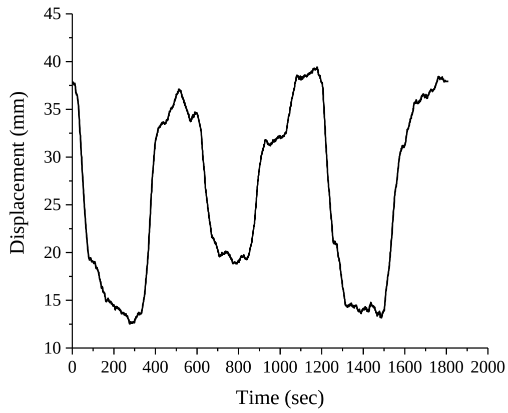

Fig. 6 Displacement vs. Time in cold working

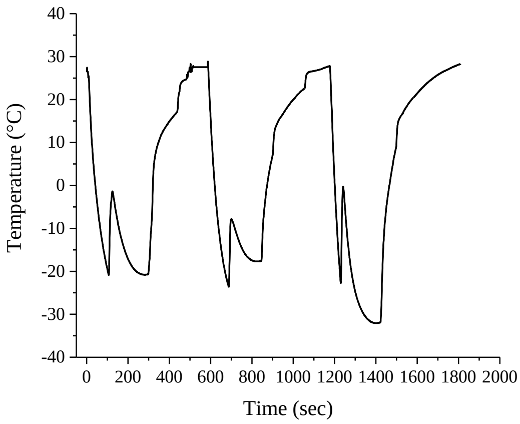

Fig. 7 Temperature vs. Time in cold working

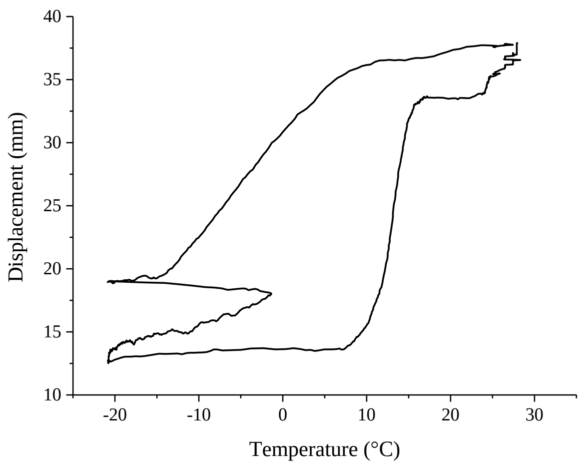

Fig. 8 Displacement vs. Temperature in cold working

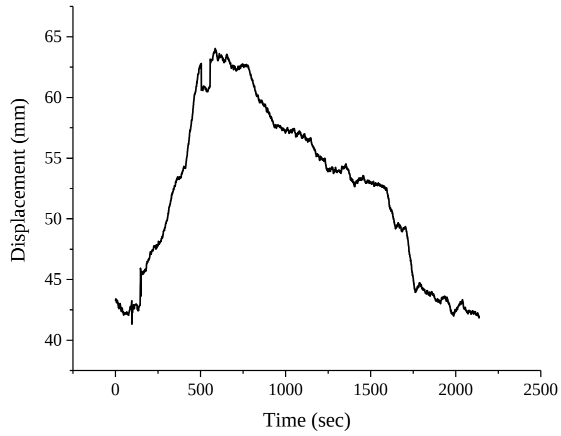

Fig. 9 Displacement vs. Time in hot working

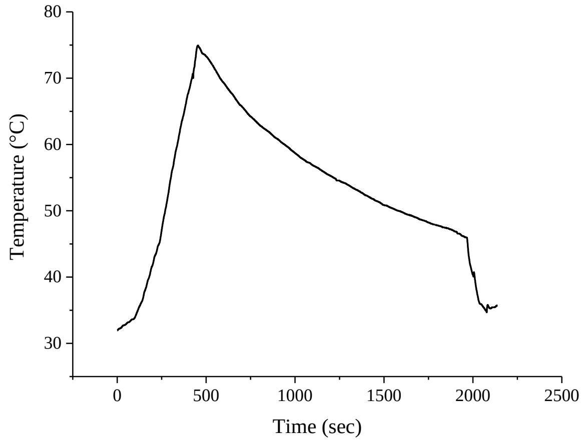

Fig. 10 Temperature vs. Time in hot working

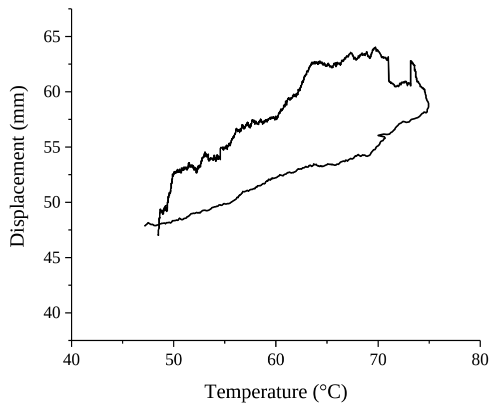

Fig. 11 Displacement vs. Temperature in hot working

the laboratory-based experimental set-up.

The results are obtained using the same procedure as discussed earlier and presented in Figs. 6-8. The total time for each cycle in case of cold working is 18.68 min (1121 sec) where the cooling is attained via liquid nitrogen and the heating is achieved by natural convection. In addition, the time taken for cooling is 3.36 min (202 s) and for the heating is 15.31 min (919 s). As the cooling is achieved via liquid nitrogen, the time taken is much lesser compared to heating. The maximum displacement is 25 mm at a load of 7N can be seen in Fig. 6. The room temperature is 28 (°C) and the lowest temperature achieved by the SMA is -33°C in the third cycle can be seen in Fig. 7. The speed of actuation of different loads is not studied in the present work. During heating there is a drastic increase in the displacement when the temperature is ranging between 8°C to 18°C, the hysteresis curve is shown in Fig. 8.

3.2 Hot water actuation

In this section, the experiments are performed on SMA wire for 7N mechanical loading via hot water bath using the laboratory-based experimental set-up.

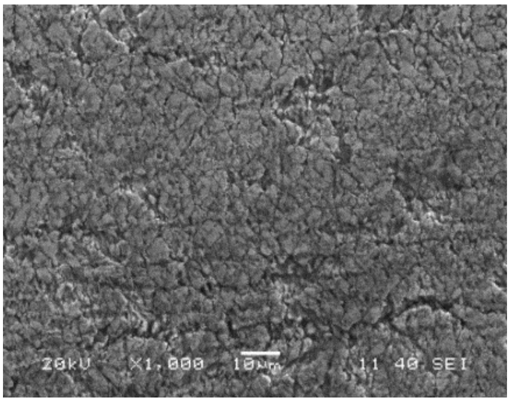

Without treatment

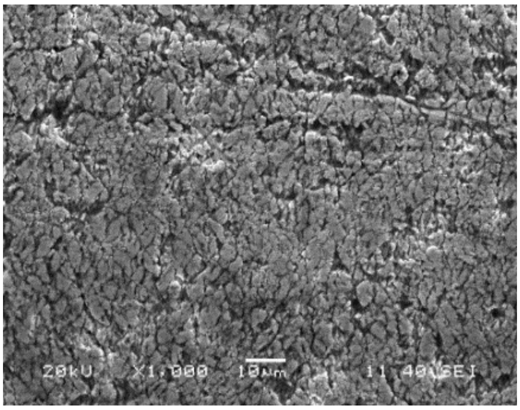

Heating

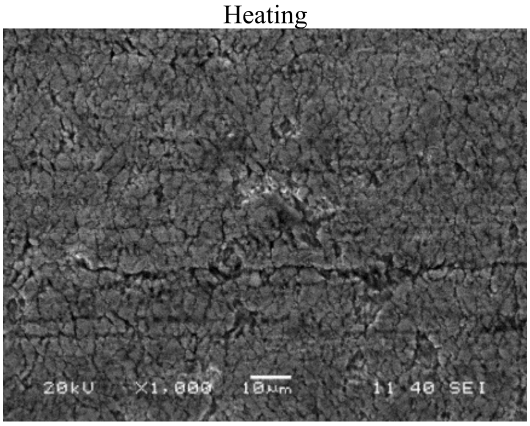

Cooling

Fig. 12 SEM images of the SMA wire for grain size

The results are obtained using the same procedure as discussed earlier and presented in Figs. 9-11. It is important to mention that the time taken the single cycle is very high as compared to the cold working i.e., liquid nitrogen actuation, hence, only one cycle is performed in this case. The total cycle time is 35.63 min (2138 s) which includes the heating time of 7.56 min (454 s) and the cooling time of 28.06 min (1684 s). As mentioned earlier, the heating is achieved via an external heat source and the cooling is done by natural convection, therefore, the time taken for the cooling is higher than the heating. It is noticed from the Fig. 9 that the maximum displacement is 20 mm at a load of 7N. Also, it is observed from the Fig. 10 that the maximum temperature allowed is 75°C. The hysteresis curve is shown in Fig. 11 and it can be seen that the temperature is ranging between 50°C to 75°C.

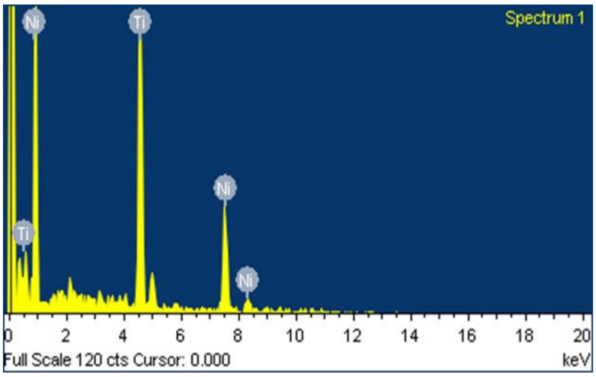

(a) Wire 1

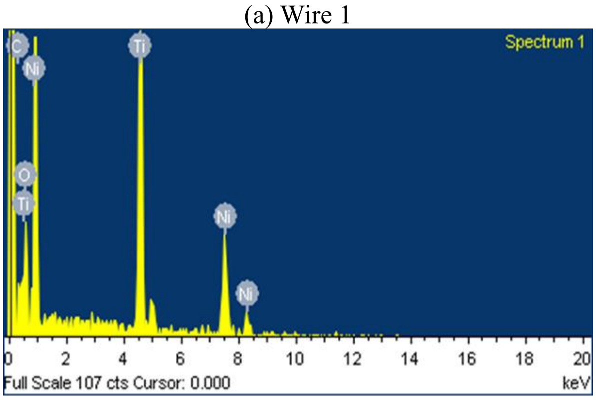

(b) Wire 2

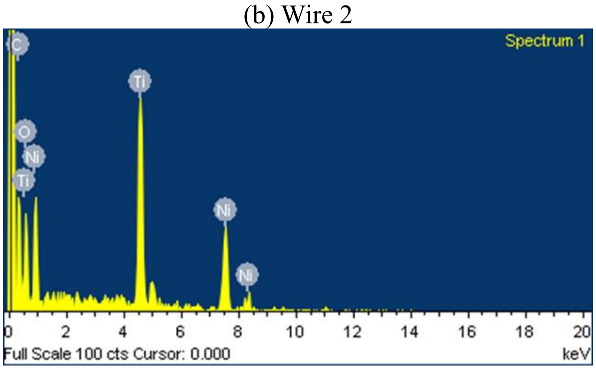

(c) Wire 3

Fig. 13 SEM images of SMA wires in spectrum form

3.3 Grain structure of SMA wires

In order to check the grain structure of the SMA wires, an experiment is conducted via SEM available at Metallurgy department, National Institute of Technology Rourkela, India. The experiment of SMA wire is performed without any actuation as well as after the actuation i.e., liquid nitrogen actuation and hot water actuation. The grain size of the SMA wires are obtained using SEM and the images are presented in Fig. 12. It is observed from the Fig. 12 that the grain size is decreasing after the liquid nitrogen actuation whereas the grain size is increasing after the hot water actuation.

3.4 Behaviour of SMA in ice, atmosphere, and boiling water

After performing the TMC experiments using the liquid nitrogen actuation and hot water actuation, another sets of experiments are performed in different conditions which are

Table 1 Composition of different SMA wires

SMA Wires		Elements			
		C	O	Ti	Ni
Wire 1	Weight%	-	-	42.53	57.47
	Atomic%	-	-	47.56	52.44
Wire 2	Weight%	15.17	16.40	33.38	35.05
	Atomic%	35.26	28.62	19.45	16.66
Wire 3	Weight%	24.58	16.79	23.78	34.85
	Atomic%	48.88	25.07	11.86	14.18

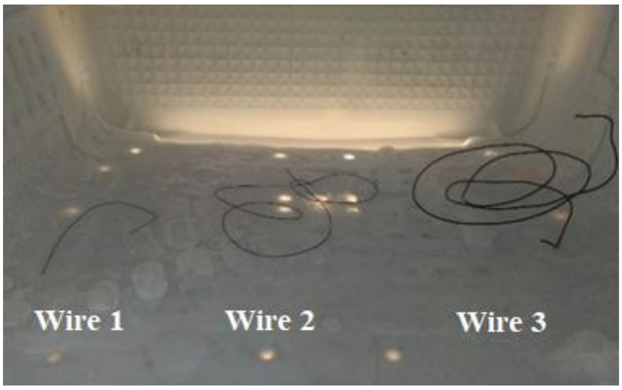

Fig. 14 SMA's at deep freezer (-15°C)

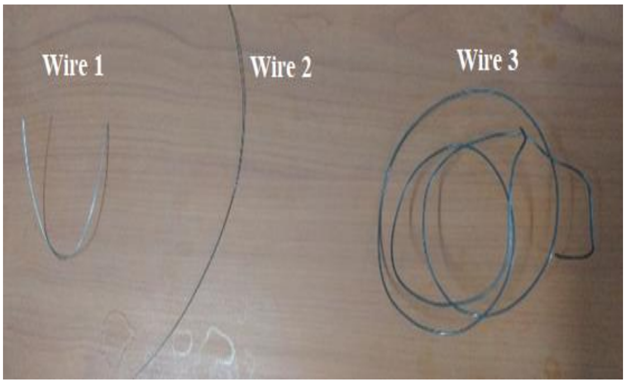

Fig. 15 SMA's at room temperature (32°C)

discussed here. The experiment is extended to analyse the behaviour of three different compositions of the SMA under different environmental conditions. In order to do so, as a first step composition of the SMA wires has been checked via SEM and the presented in Table 1 which shows the content of carbon (C), oxygen (O), titanium (Ti) and nickel (Ni). In addition, the SEM study is presented in spectrum form in Fig. 13.

As a next step, the SMA wires of different composition have been kept in the deep freezer as shown in Fig. 14 and they were deformed manually. It is noticed that out of three wires, the first wire (wire 1) unable to deform whereas other two wires (wire 2 and wire 3) deforming easily. Hence, the experiment indicates that the wire 2 and the wire 3 are in their unstable temperature state i.e., the martensite phase attains at -15°C (deep freezer) whereas the wire 1 is at the stable state (Austenite).

After performing the cooling test, all three wires are

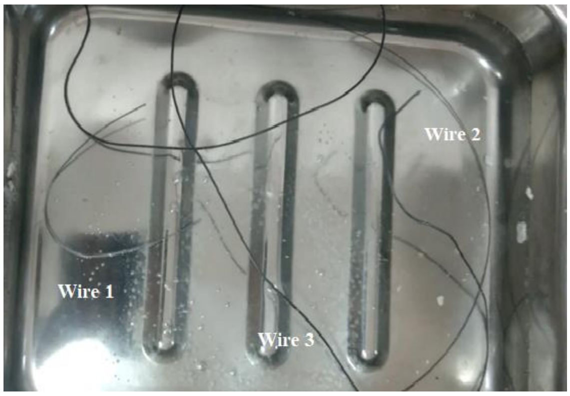

Fig. 16 SMA's at the hot water (95°C)

exposed to the ambient condition (32°C) and the deformation (actuation) process observed for the wire 2. The change in temperature indicates the initiation of the phase transformation process for the wire 2. Additionally, it is interesting to note that the wire 2 regaining the original shape but too slow. However, the wire 1 and wire 3 are showing no deformation because of their Austenite and Martensite state (refer Fig. 15) of temperature at the deep freezer and the room temperature, respectively. Finally, the experiment is carried out by placing all three SMA wires in hot water bath as shown in Fig. 16. It is observed from the fig, that the third wire also started to undergo deformation that means the change or regaining back to its original shape and all the wires are at stable state i.e., Austenite phase and can be seen in Fig. 16.

Based on the above SEM study and the behaviour in different environmental condition, it is observed that the wire 1 without any carbon and oxygen contents has the austenite temperature that is lower than the temperature in the deep freezer (-15°C). In addition, the wire 2 having the carbon and the oxygen of 31.57% has austenite phase change is at room temperature (32°C). Moreover, the wire 3 having the carbon and the oxygen of 41.37% has austenite phase change is at a higher temperature (95°C). Therefore, it is understood from the above analysis that the percentage of the carbon and the oxygen increases as well as the percentage of the nickel and the titanium decreases than the austenite phase temperature increases.

4. Conclusions

A lab-scale experimental set-up has been developed for the experimentation to examine the thermo-mechanical loading on commercial SMA wires. In this regard, heating and cooling effect have been achieved using the liquid nitrogen and hot water actuation. After the solid-state phase change the molecular rearrangement of the utilized SMA wires are verified before and after the TMC with the help of SEM. The experimentation was carried out on three different types of the SMA wires and compositional effect on the thermomechanical loading also discussed for the sake of clarification. All three different SMA wires engaged in the experimental analysis infers different characteristics under the variable environment, i.e., low temperature, room temperature and at high-temperature. The result shows that the SMA wire in its Martensite phase acts like a normal wire i.e., it experiences expansion including the contraction on heating and cooling cycles whereas the activated behavior observed during the high-temperature Austenite phase. Additionally, the study reveals that the wire commercially available may not follow the expected line while the alloy deviates from the equiatomic configuration, i.e., consist of foreign impurities (carbon or oxygen). Finally, it is understood that the phase transformation temperature and the cyclic load-bearing capacity largely depends on the alloy composition.

References

Abdelbaki, C., Bakora, A., Houari, H., Houari, M.S.A., Tounsi, A. and Bedia, E.A.A. (2016b), "Thermo-mechanical postbuckling of symmetric S-FGM plates resting on Pasternak elastic foundations using hyperbolic shear deformation theory", *Struct. Eng. Mech.*, **57**(4), 617-639.

Amnieh, H.B., Zamzam, M.S. and Kolahchi, R. (2018), "Dynamic analysis of non-homogeneous concrete blocks mixed by SiO_2 nanoparticles subjected to blast load experimentally and theoretically", *Constr. Build. Mater.*, **174**, 633-644.

Antunes, A.S., Santos, O.S., Naito, L.K.F., Rigo, O.D. and Otubo, J. (2018), "The wire drawing mechanics of near-equiatomic NiTi SMA", *Mater. Res.*, **21**(3), e20170944.

Arani, A.G., Kolahchi, R. and Barzoki, A.A.M. (2011), "Effect of material in-homogeneity on electro-thermo-mechanical behaviors of functionally graded piezoelectric rotating shaft", *Appl. Math. Modell.*, **35**, 2771-2789.

Arani, A.J. and Kolahchi, R. (2016), "Buckling analysis of embedded concrete columns armed with carbon nanotubes", *Comput. Concrete*, **17**(5), 567-578.

Attia, A., Bousahla, A.A., Tounsi, A., Mahmoud, S.R. and Alwabli, A.S. (2018), "A refined four variable plate theory for thermoelastic analysis of FGM plates resting on variable elastic foundations", *Struct. Eng. Mech.*, **65**(4), 453-464.

Barka, M., Benrahou, K.H., Bakora, A. and Tounsi, A. (2016a), "Thermal post-buckling behavior of imperfect temperature-dependent sandwich FGM plates resting on Pasternak elastic foundation", *Struct. Eng. Mech.*, **22**(1), 91-112.

Barzoki, A.A.M., Arani, A.G., Kolahchi, R. and Mozdianfard, M.R. (2012), "Electro-thermo-mechanical torsional buckling of a piezoelectric polymeric cylindrical shell reinforced by DWBNNTs with an elastic core", *Appl. Math. Modell.*, **36**, 2983-2995.

Baseri, V., Jafari, G.S. and Kolahchi, R. (2016), "Analytical solution for buckling of embedded laminated plates based on higher order shear deformation plate theory", *Steel Compos. Struct.*, **22**(4), 889-913.

Beldjelili, Y., Tounsi, A. and Hassan, S. (2016c), "Hygro-thermo-mechanical bending of S-FGM plates resting on variable elastic foundations using a four-variable trigonometric plate theory", *Smart Struct. Syst.*, **18**(4), 755-786.

Bhagyaraj, J., Ramaiah, K.V., Saikrishna, C.N., Gouthama. and Bhaumik, S.K. (2013), "Behavior and effect of Ti2Ni phase during processing of NiTi shape memory alloy wire from cast ingot", *J. Alloys Compd.*, **581**, 344-351.

Bhaumik, S.K., Saikrishna, C.N., Ramaiah, K.V. and Venkataswamy, M.A. (2008), "Understanding the fatigue behaviour of NiTiCu shape memory alloy wire thermal actuators", *Key Eng. Mater.*, **378-379**, 301-316.

Bilouei, B.S., Kolahchi, R. and Bidgoli, M.R. (2016), "Buckling of concrete columns retrofitted with nano-fiber reinforced polymer (NFRP)", *Comput. Concrete*, **18**(5) 1053-1063.

Bouderba, B., Houari, M.S.A., Tounsi, A. and Hassan, S. (2016), "Thermal stability of functionally graded sandwich plates using a simple shear deformation theory", *Struct. Eng. Mech.*, **58**(3), 397-422.

Bousahla, A.A., Benyoucef, S., Tounsi, A. and Samy Hassan, S. (2016), "On thermal stability of plates with functionally graded coefficient of thermal expansion", *Struct. Eng. Mech.*, **60**(2), 313-335.

Chikh, A., Tounsi, A., Hebali, H. and Mahmoud, S.R. (2017), "Thermal buckling analysis of cross-ply laminated plates using a simplified HSDT", *Smart Struct. Syst.*, **19**(3), 289-297.

Churchill, C.B. and Shaw, J.A. (2008), "Shakedown response of conditioned shape memory alloy wire", *Proceedings of the Behavior and Mechanics of Multifunctional and Composite Materials*, **6929**, 69291F-1-12.

Cuellar, E.L., Pavon, L.L., Mendoza, E.N., Araujo, C.J.D., Castro, W.B.D., Gonzalez, C. and Otubo, J. (2016), "Effect of spun velocities and composition on the microstructure and transformation temperatures of TiNi shape memory ribbons", *Mater. Re.*, **19**(5), 1132-1137.

Eggeler, G., Hornbogen, E., Yawny, A., Heckmann, A. and Wagner, M. (2004), "Structural and functional fatigue of NiTi shape memory alloys", *Mater. Sci. Eng. A.*, **378**(1-2), 24-33.

El-Haina, F., Bakora, A., Bousahla, A.A., Tounsi, A. and Mahmoud, S.R. (2017), "A simple analytical approach for thermal buckling of thick functionally graded sandwich plates", *Struct. Eng. Mech.*, **63**(5), 585-595.

Erbstoeszer, B., Armstrong, B., Taya, M. and Inoue, K. (2000), "Stabilization of the shape memory effect in NiTi: An experimental investigation", *Scr. Mater.*, **42**(12), 1145-1150.

Golabchi, H., Kolahchi, R. and Bidgoli, M.R. (2018), "Vibration and instability analysis of pipes reinforced by SiO_2 nanoparticles considering agglomeration effects", *Comput. Concrete*, **21**(4), 431-440.

Hajmohammad, M.H, Kolahchi, Zarei, M.S. and Maleki, M. (2018a), "Earthquake induced dynamic deflection of submerged viscoelastic cylindrical shell reinforced by agglomerated CNTs considering thermal and moisture effects", *Compos. Struct.*, **187**, 498-508.

Hajmohammad, M.H., Farrokhian, A. and Kolahchi, R. (2018b), "Smart control and vibration of viscoelastic actuator-multiphase nanocomposite conical shells-sensor considering hygrothermal load based on layerwise theory", *Aerosp. Sci. Technol.*, **78**, 260-270.

Hajmohammad, M.H., Malekia, M. and Kolahchi, R. (2018c), "Seismic response of underwater concrete pipes conveying fluid covered with nano-fiber reinforced polymer layer", *Soil Dyn. Earthq. Eng.*, **110**, 18-27.

Hajmohammad, M.H., Zarei, M.S., Nouri, A. and Kolahchi, R. (2017), "Dynamic buckling of sensor/functionally graded-carbon nanotubes reinforced laminated plates/actuator based on sinusoidal-viscopiezoelasticity theories", *J. Sandw. Struct. Mater.*

Hamidi, A., Houari, M.S.A, Hassan, S. and Tounsi, A. (2015), "A sinusoidal plate theory with 5-unknowns and stretching effect for thermomechanical bending of functionally graded sandwich plates", *Steel Compos. Struct.*, **18**(1), 235-253.

Humbeeck, J.V. (1991), "Cycling effects, fatigue and degradation of shape memory alloys", *J. Phys. Colloq.*, **1**(C4), C4-189-C4-197.

Jiang, X., Hida, M., Takemoto, Y., Sakakibara, A., Yasuda, H. and Mori, H. (1997), "In situ observation of stress-induced martensitic transformation and plastic deformation in TiNi alloy", *Mater. Sci. Eng. A.*, **238**(2), 303-308.

Karami, B., Janghorban, M., Shahsavari, D. and Tounsi, A. (2018), "A size-dependent quasi-3D model for wave dispersion analysis of FG nanoplates", *Steel Compos. Struct.*, **28**(1), 99-110.

Khetir, H., Bouiadjra, M.B., Houari, M.S.A., Tounsi, A. and Hassan, S.R. (2017), "A new nonlocal trigonometric shear deformation theory for thermal buckling analysis of embedded nanosize FG plates", *Struct. Eng. Mech.*, **64**(4), 391-402.

Kolahchi, R. (2017), "A comparative study on the bending, vibration and buckling of viscoelastic sandwich nano-plates based on different nonlocal theories using DC, HDQ and DQ methods", *Aerosp. Sci. Technol.*, **66**, 235-248.

Kolahchi, R. and Bidgoli, A.M.M. (2016), "Size-dependent sinusoidal beam model for dynamic instability of single-walled carbon nanotubes", *Appl. Math. Mech.-Engl. Ed.*, **37**(2), 265-274.

Kolahchi, R. and Cheraghbak, A. (2017), "Agglomeration effects on the dynamic buckling of viscoelastic microplates reinforced with SWCNTs using Bolotin method", *Nonlin. Dyn.*, **90**, 479-492.

Kolahchi, R. Keshtegar, B. and Fakhar, M.H. (2017b), "Optimization of dynamic buckling for sandwich nanocomposite plates with sensor and actuator layer based on sinusoidalvisco-piezoelasticity theories using Grey Wolf algorithm", *J. Sandw. Struct. Mater.*

Kolahchi, R., Hosseini, H. and Esmailpour, M. (2016a), "Differential cubature and quadrature-Bolotin methods for dynamic stability of embedded piezoelectric nanoplates based on visco-nonlocal-piezoelasticity theories", *Compos. Struct.*, **157**, 174-186.

Kolahchi, R., Safari, M. and Esmailpour, M. (2016b), "Dynamic stability analysis of temperature-dependent functionally graded CNT-reinforced visco-plates resting on orthotropic elastomeric medium", *Compos. Struct.*, **150**, 255-265.

Kolahchi, R., Zarei, M.S., Hajmohammad, M.H. and Nouri, A. (2017a), "Wave propagation of embedded viscoelastic FG-CNT-reinforced sandwich plates integrated with sensor and actuator based on refined zigzag theory", *Int. J. Mech. Sci.*, **130**, 534-545,

Kolahchi, R., Zarei, M.S., Hajmohammad, M.H. and Oskouei, A.N. (2017c), "Visco-nonlocal-refined Zigzag theories for dynamic buckling of laminated nanoplates using differential cubature-Bolotin methods", *Thin Wall. Struct.*, **113**, 162-169.

Koomen, T.J. (2015), "General control framework for shape memory alloy based aatuators-a phase transformation approach", M.Sc. Dissertation, Delft University of Technology, Delft, the Netherlands.

Liu, Y., Xie, Z. and Humbeeck, J.V. (1999), "Cyclic deformation of NiTi shape memory alloys", *Mater. Sci. Eng. A.*, 273-357, 673-678.

Lobo, P.S., Almeida, J. and Guerreiro, L. (2015), "Shape memory alloys behaviour", *Rev. Proc. Eng.*, **114**, 776-783.

Menasria, A., Bouhadra, A., Tounsi, A., Bousahla, A.A. and Mahmoud, S.R. (2017), "A new and simple HSDT for thermal stability analysis of FG sandwich plates", *Steel Compos. Struct.*, **25**(2), 157-175.

Mouffoki, A., Bedia, E.AA., Houari, M.S.A., Tounsi, A. and Mahmoud, S.R. (2017), "Vibration analysis of nonlocal advanced nanobeams in hygro-thermal environment using a new two-unknown trigonometric shear deformation beam theory", *Smart Struct. Syst.*, **20**(3), 369-383.

Nath, T., Chouhan, P., Disawal, R. and Palani, I.A. (2017), "Comparative study of electrically and hot water actuated shape memory alloy using developed thermo-mechanical cycle test bench", *Def. Sci. J.*, **67**(1), 101-107.

Perkins, J. and Sponholz, R.O. (1984), "Stress-induced martensitic transformation cycling and two-way shape memory training in Cu-Zn-Al alloys", *Metall. Trans. A.*, **15**(2), 313-321.

Ramaiah, K.V., Saikrishna, C.N., Dhananjaya, B.R. and Bhaumik, S.K. (2005), "Effects of thermo-mechanical cycling on the functional properties of Ni-Ti-Cu shape memory alloys", *Proceedings of the International Conference on Smart Materials, Structures, and Systems*.

Saikrishna, C.N., Ramaiah, K.V. and Bhaumik, S.K. (2006), "Effects of thermo-mechanical cycling on the strain response of Ni-Ti-Cu shape memory alloy wire actuator", *Mater. Sci. Eng. A.*, **428**(1-2), 217-224.

Saikrishna, C.N., Ramaiah, K.V., Prabhu, S.A. and Bhaumik, S.K. (2001), "On stability of NiTi wire during thermo-mechanical cycling", *Bull. Mater. Sci.*, **32**(3), 343-352.

Stachowiak, G.B. and McCormick, P.G. (1988), "Shape memory behaviour associated with the R and martensitic transformations in a NiTi alloy", *Acta Metall.*, **36**(2), 291-297.

Stalmans, R., Humbeeck, J.V. and Delaey, L. (1991), "Training and the two-way memory effect in copper-based shape memory alloys", *J. Phys. Colloq.*, **1**(C4), C4-403-C4-408.

Stosic, Z., Manasijevic, D., Balanovic, L., Holjevac-Grguric, T., Stamenkovic, U., Premovic, M., Minic, D., Gorgievski, M. and Todorovic, R. (2017), "Effects of composition and thermal treatment of Cu-Al-Zn alloys with low content of Al on their shape-memory properties", *Mater. Res.*, **20**(5), 1425-1431.

Taghizadeh, M., Ovesy, H.R. and Ghannadpour, S.A.M. (2015), "Nonlocal integral elasticity analysis of beam bending by using finite element method", *Struct. Eng. Mech.*, **54**(4), 755-769.

Totounferoush, A., Ovesy, H.R. and Ghannadpour, S.A.M. (2014) "Nonlinear dynamic buckling response analysis of piezo-composite plates subjected to in-plane loads", *Proceedings of the 4th International Conference on Acoustics & Vibration (ISAV2014)*, Tehran, Iran, December.

Uchil, J., Mohanchandra, K.P., Kumara, K.G., Mahesh, K.K. and Murali, T.P. (1999), "Thermal expansion in various phases of Nitinol using TMA", *Phys. B*, **270**(3-4), 289-297.

Zamanian, M., Kolahchi, R. and Bidgoli, M.R. (2017), "Agglomeration effects on the buckling behaviour of embedded concrete columns reinforced with SiO_2 nano-particles", *Wind Struct.*, **24**(1), 43-57.

Zarei, M.S., Kolahchi, R., Hajmohammad, M.H. and Maleki, M. (2017), "Seismic response of underwater fluid-conveying concrete pipes reinforced with SiO_2 nanoparticles and fiber reinforced polymer (FRP) layer", *Soil Dyn. Earthq. Eng.*, **103**, 76-85.

CC